JOURNAL OF SPACECRAFT AND ROCKETS
Vol. 42, No. 4, July–August 2005

Through-Thickness Connection of Matrix Cracks in Laminate Composites for Propellant Tank

Tomohiro Yokozeki* and Takashi Ishikawa†
Japan Aerospace Exploration Agency, Tokyo 181-0015, Japan
and
Takahira Aoki‡
University of Tokyo, Tokyo 113-8656, Japan

Matrix crack accumulation in multiple plies of composite laminates is experimentally investigated to assess the through-thickness connection of matrix cracks, which is closely related to propellant leakage problems of composite tanks. Cracking patterns in $[0/\theta_2/90]_s$ laminates reveal that layup angles have a significant effect on crack induction mechanisms in contiguous plies. Matrix crack propagation behaviors in the fiber direction of θ ply induced by 90-ply cracks are investigated in terms of energy release rates using parametric-oriented finite element analysis based on an oblique coordinate system. The effect of cryogenic conditions on crack induction in contiguous plies is also studied, and discussions on through-thickness connection of matrix cracks in composite laminates are provided.

Nomenclature

a	=	crack length in θ-deg ply projected to $\bar{x}$ coordinate
$\boldsymbol{g}_1, \boldsymbol{g}_2, \boldsymbol{g}_3$	=	covariant base vectors of oblique coordinates
$\boldsymbol{g}^1, \boldsymbol{g}^2, \boldsymbol{g}^3$	=	contravariant base vectors of oblique coordinates
G_1, G_2	=	energy release rate
$\boldsymbol{i}_1, \boldsymbol{i}_2, \boldsymbol{i}_3$	=	base vectors of orthogonal coordinates
l_x	=	crack spacing of 90 ply projected to orthogonal coordinates
l_y	=	crack spacing of θ ply projected to orthogonal coordinates
R	=	ratio of applied strain, $\hat{\bar{\varepsilon}}_y/\hat{\bar{\varepsilon}}_x$
t_θ	=	thickness of θ-deg ply
u, v, w	=	covariant components of displacement along oblique coordinates
x, y, z	=	oblique coordinates
$\bar{x}, \bar{y}, \bar{z}$	=	orthogonal coordinate
$\hat{\varepsilon}_{ij}$	=	covariant components of prescribed strain in the oblique coordinates
$\hat{\bar{\varepsilon}}_{ij}$	=	prescribed strain in the oblique coordinates
ρ_1	=	matrix crack density in θ ply
ρ_2	=	matrix crack density in 90 ply

Introduction

COMPOSITE laminates are the major candidates for reducing the structural weight of future reusable launch vehicles (RLV). Particularly, the application of carbon fiber-reinforced plastic laminates to the cryogenic propellant tanks is one of the most desired but challenging technologies for achieving drastic weight reduction of RLV.[1,2] Basic research on the feasibility of cryogenic composite propellant tanks indicates that matrix crack onset and its accumulation are inevitable when applying the conventional high-performance composites to the cryogenic tanks and that multiple-ply matrix cracks may induce crucial propellant leakage.[3–5] Because of this, the damage process of crack accumulation in multiple plies has to be clarified to provide an adequate guideline for cryogenic composite tank design.

Matrix cracking in laminated structures subjected to thermomechanical loadings has been extensively studied in both theoretical and experimental frameworks.[6,7] Recently, many researchers have been actively engaged in characterization of stiffness, strength, and matrix cracking behaviors under cryogenic conditions.[8,9] However, compared to the crack accumulation in a single-ply block, crack formation in multiple plies has not yet been studied thoroughly. In past experimental research, matrix crack accumulation could be observed in all plies of laminates, for example, quasi-isotropic laminates containing 0-, ±45-, and 90-deg plies, especially under cyclic loadings.[10–12] One of the characteristic damage modes is crack-induced microcrack or stitch crack in plies adjacent to the ply containing transverse cracks.[11,12] Following the developed matrix crack accumulation in a single-ply block of the laminate, stitch cracks may be induced in the adjacent plies (and instantaneous numerous formations occasionally take place). However, most considerations on multiple-ply crack accumulation assume formation of developed cracks on initiation. Thus, it is inevitable that the susceptibility of microcrack propagation in the fiber direction in the plies adjacent to the ply containing traversing matrix cracks and the mechanisms of adjacent-ply cracking have to be investigated for the consideration of the durability of composite tank structures.

In this study, matrix crack accumulation in multiple plies of composite laminates is experimentally investigated to assess through-thickness connection of matrix cracks in composite laminates. Specifically, the effect of laminate configuration, for example, layup angle, on crack-induction mechanisms in contiguous plies is investigated. To clarify the damage mechanisms, parametric-oriented finite element analyses are performed for the stress calculation of obliquely crossed cracked laminates. Susceptibility to stitch cracks or developed cracks is analyzed by calculating energy release rates associated with θ-ply crack growth in the fiber direction of $[0/\theta_2/90]_s$ laminates. The effect of cryogenic conditions on crack induction in contiguous plies is also studied, and comments on through-thickness connection of matrix cracks in composite laminates are presented.

Experimental

To study the mechanisms of matrix cracking in multiple plies, an experimental investigation of $[0/\theta_2/90]_s$ laminates is made. In particular, the focus is on the crack accumulation process in the θ ply in

Presented as Paper 2004-1772 at the AIAA/ASME/ASCE/AHS/ASC 45th Structures, Structural Dynamics, and Materials Conference, Palm Springs, CA, 19–22 April 2004; received 27 May 2004; revision received 10 August 2004; accepted for publication 13 August 2004.

*Researcher, Advanced Composite Evaluation Technology Center, Institute for Space Technology and Aeronautics, Mitaka. Member AIAA.
†Director, Advanced Composite Evaluation Technology Center, Institute for Space Technology and Aeronautics, Mitaka. Member AIAA.
‡Professor, Department of Aeronautics and Astronautics. Member AIAA.

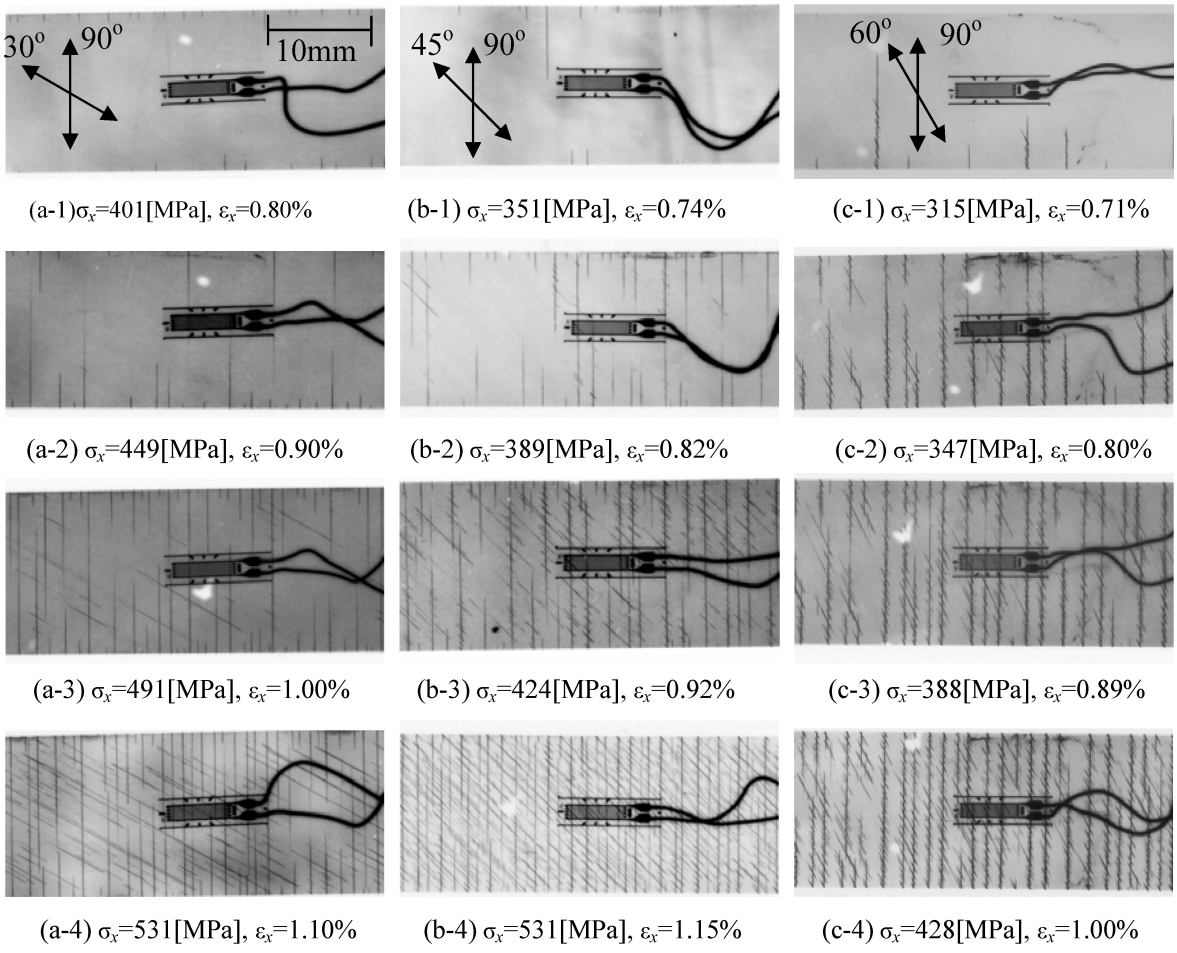

Fig. 1 Matrix cracking behaviors in multiple plies in $[0/\theta_2/90]_s$ laminate: a) $[0/30_2/90]_s$, b) $[0/45_2/90]_s$, and c) $[0/60_2/90]_s$.

the presence of 90-ply cracks. The reason that unbalanced laminates are chosen for this study, as opposed to balanced laminates commonly utilized, should be noted. The effect of layup angles on crack induction mechanisms in contiguous plies is mainly investigated in this study. Therefore, laminates in which matrix cracks would not be induced in more than two plies, that is, θ and 90 plies, are chosen. In addition, free-edge delaminations, which affect the matrix crack accumulation process, are susceptible to initiation in balanced coupon specimens,[13] for example, $[\theta/-\theta/90]_s$ and $[0/\theta/-\theta/90]_s$. Considering that tank structures have no free edges, we chose the unbalanced laminates to prevent free-edge delaminations during tensile loadings.

Three types of coupon specimens of $[0/30_2/90]_s$, $[0/45_2/90]_s$, and $[0/60_2/90]_s$ were prepared. The material system is IM600/133, an intermediate-modulus carbon fiber and toughened epoxy system. All specimens were 250 mm long with 50-mm glass fiber-reinforced plastic end tabs, leaving a 150-mm gauge section. Because of the shear–extension coupling of the entire laminate characteristics, the specimen width affects the uniformity of the stress field. Although the usage of specimens with thin width or oblique end tabs[14] is preferable, the specimen width was configured to be 15 mm to assure that there are enough regions of uniform deformation, which was verified by finite element analysis. Therefore, we set the central regions of the 40-mm-long specimens as the observed regions of matrix cracks.

Quasi-static tensile tests were performed using an Instron 8802 hydraulic-driven loading machine at a crosshead speed of 0.5 mm/min at room temperature. Strain gauges were attached to the specimens to measure axial strains. When the specimens were loaded to the predetermined strain levels, zinc iodide penetrant was applied to the free edges, and the specimens were held for 5 min. The specimens were removed from the machine, and soft x-ray radiography (soft x-ray transmission method) was conducted on the cracked specimens to check cracking patterns. These specimens were then loaded to the next strain levels. Repeating these steps, cracking patterns in $[0/\theta_2/90]_s$ laminates were obtained as a function of applied laminate strains.

In Fig. 1, the θ-ply cracking configuration in the presence of 90-ply cracks when $\theta = 30$, 45, and 60 deg is shown. Note that numerous θ-ply microcracks (stitch cracks) could be observed in the $[0/45_2/90]_s$ and $[0/60_2/90]_s$ laminates when 90-ply cracks initiated and extended in the fiber direction. At higher strain levels, microcracks increased in number in conjunction with the 90-ply crack increase. In contrast, stitch cracks were rarely observed in the $[0/30_2/90]_s$ laminates and the 30-ply cracks appeared as developed cracks. These results indicate that the intersecting angle between the contiguous cracked plies, that is, 90 and θ ply has significant effects on the process of θ-ply crack formation. When the intersecting angle is small, stitch cracks are observed before propagation in the fiber direction as is the case for $\theta = 45$ and 60 deg. However, developed cracks mainly form in the cases of large intersecting angles.

Matrix cracking in the outer 0-deg plies was also observed when applied loads increased. Figure 2 indicates matrix crack accumulation in all of the constituent plies of $[0/30_2/90]_s$ and $[0/60_2/90]_s$ laminates. Matrix cracks were induced consecutively once the first-ply cracking was observed in the order 90, θ, and then 0 ply.

For further investigation, the x-ray computerized tomography scanning technique was applied to the specimens using TOSCARNER-30000 μhd (Toshiba Corp.). Cross-sectional images perpendicular to the axial direction (0-deg direction) of cracked laminates with scanning intervals of 0.2 mm were obtained as shown in Fig. 3. The numbers of observed matrix cracks in θ-deg plies above and below the 90-deg ply are almost equal to each other. Matrix cracks in 0-deg plies can also be observed in Fig. 3.

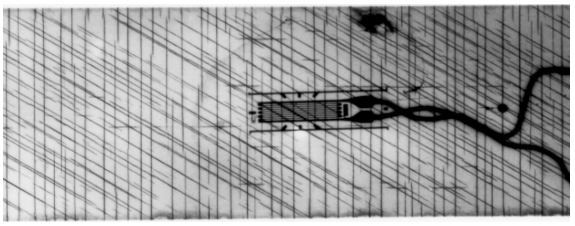

a) $[0/30_2/90]_s$, $\sigma_x = 572$ MPa, $\varepsilon_x = 1.22\%$

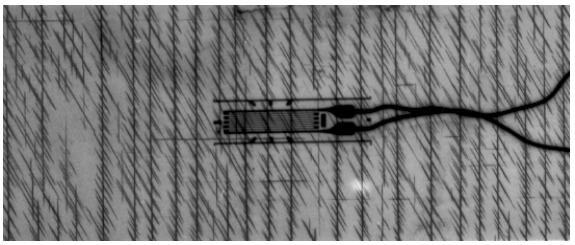

b) $[0/60_2/90]_s$, $\sigma_x = 534$ MPa, $\varepsilon_x = 1.25\%$

Fig. 2 Through-thickness connections of matrix cracks.

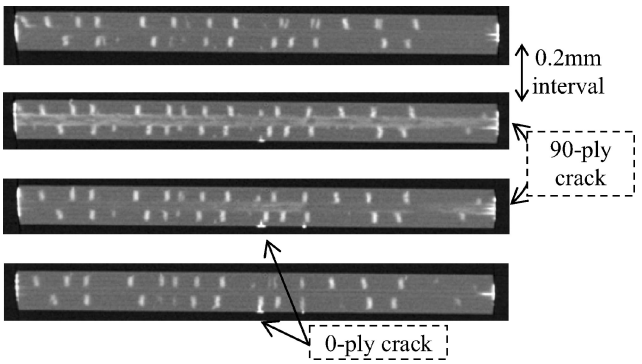

Fig. 3 Sequential CT scanning images perpendicular to 0-deg direction of cracked laminates.

Analytical Modeling

Consider a $[S/\theta_m/90_n]_s$ laminate containing obliquely crossed cracks, that is, θ- and 90-ply cracks, where S is a sublaminate. To discuss stress distributions and boundary settings, it is appropriate to utilize an oblique coordinate system along the θ- and 90-ply cracks. Therefore, obliquely crossed base vectors are introduced herein to permit parametric analysis for angle θ under the conditions of constant obliquely crossed crack densities (or crack spacings), as discussed in a previous study.[15]

Let r_1 and r_2 be reference lines along the θ- and 90-ply fiber directions, that is, crack propagation directions, respectively. The base vectors $\boldsymbol{g}_1$, $\boldsymbol{g}_2$, and $\boldsymbol{g}_3$ are set along the coordinate lines r_1, r_2 and the line perpendicular to the plane formed by the lines r_1 and r_2 as shown in Fig. 4. Base vectors of an orthogonal coordinate system along the 0- and 90-ply fiber direction utilized in the common stress analysis are defined as $\boldsymbol{i}_1$, $\boldsymbol{i}_2$, and $\boldsymbol{i}_3$, as shown in Fig. 4. The coordinate systems based on $\boldsymbol{g}_i$ and $\boldsymbol{i}_i$ are denoted as x–y–z oblique coordinates and $\bar{x}$–$\bar{y}$–$\bar{z}$ orthogonal coordinates, respectively.

In this study, base vectors $\boldsymbol{g}_i$ are set so that all contravariant base vectors $\boldsymbol{g}^i$ have unit length because of the tractability for parametric studies based on the variable angle θ under the conditions of identical oblique crack densities. The covariant base vectors $\boldsymbol{g}_i$ are expressed in terms of orthogonal coordinate components as

$$\boldsymbol{g}_1 = (1, \tan\theta, 0), \qquad \boldsymbol{g}_2 = (0, \sec\theta, 0), \qquad \boldsymbol{g}_3 = (0, 0, 1) \quad (1)$$

Based on these base vectors, a finite element formulation was developed in a previous study.[15] When this formulation is used, parametric stress analysis for angle θ of obliquely crossed cracked laminates is performed.

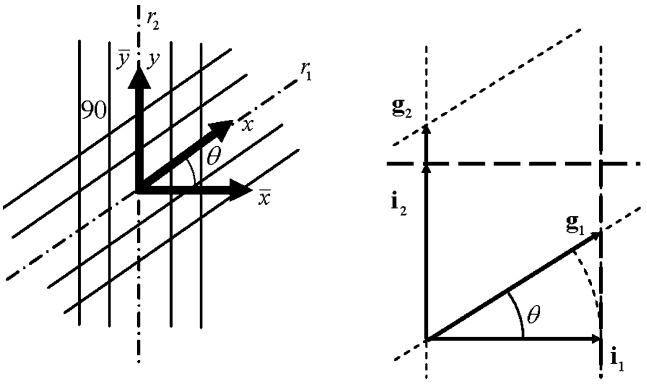

Fig. 4 Base vectors of oblique and orthogonal coordinate systems.

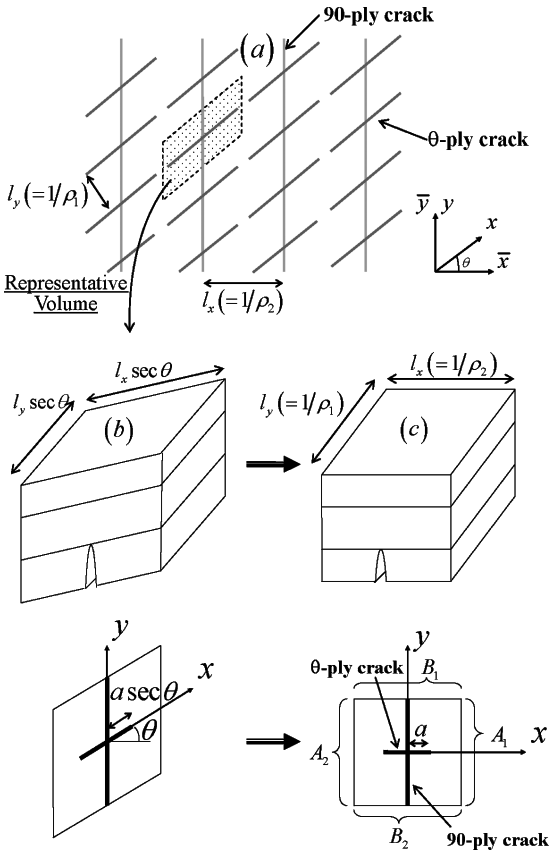

Fig. 5 Laminate model containing obliquely crossed cracks to be analyzed.

To investigate the induction mechanisms of matrix cracks in contiguous plies, $[0/\theta_2/90]_s$ laminates containing θ- and 90-ply cracks are analyzed utilizing the just mentioned transformation modeling. It is assumed that 1) 90-ply cracks are developed completely in the fiber direction and are regularly arranged with a uniform crack spacing of l_x; 2) θ-ply cracks are located symmetrically with respect to the middle surface, all of which have the length $2a$ propagating equally in the fiber direction from the 90-ply cracks and a uniform crack spacing of l_y; and 3) the θ-ply crack tips are straight along the thickness direction. The configuration of the assumed model is shown in Fig. 5a. Thus, the representative volume to be analyzed can be taken as Fig. 5b and geometrically modeled in the orthogonal shape as Fig. 5c, in which covariant displacement/strain components, contravariant force/stress components, and the related stiffness are applied. The model with orthogonal geometry can be used for any angle θ under the conditions of identical crack densities.

In the model of Fig. 5c, boundary conditions at the corresponding nodes on the surfaces across the x and y axes should be

Table 1 Material properties (IM600/133) used in analysis[a]

Temperature, °C	E_L, GPa	E_T, GPa	ν_{LT}	G_{LT}, GPa	G_{TT}, GPa	α_L, μ/°C	α_T, μ/°C
100	146.4	6.3	0.36	2.2	2.2	−0.60	41.5
60	146.8	7.2	0.35	3.5	2.5	−0.45	36.0
20	147.1	8.3	0.35	4.7	2.9	−0.55	22.5
−20	147.5	9.2	0.35	5.5	3.2	−0.59	19.5
−100	148.3	11.0	0.35	6.9	3.8	−0.65	14.5
−196	149.1	12.8	0.35	7.7	4.4	−0.70	10.0
−269	150.0	14.7	0.35	8.0	5.1	−0.75	5.5

[a]Here ν_{TT} is assumed to be 0.45.

applied as

$$u^{A_1} - u^{A_2} = \hat{\varepsilon}_x l_x, \qquad v^{A_1} - v^{A_2} = \hat{\gamma}_{xy} l_x, \qquad w^{A_1} - w^{A_2} = 0$$
$$u^{B_1} - u^{B_2} = 0, \qquad v^{B_1} - v^{B_2} = \hat{\varepsilon}_y l_y, \qquad w^{B_1} - w^{B_2} = 0 \quad (2)$$

in addition to the symmetric conditions on the middle surface, where u, v, and w are covariant components of displacement along x, y, and z directions, $\hat{\varepsilon}_{ij}$ are the prescribed covariant strain components, A_i and B_i are the boundary surfaces defined in Fig. 5c, and l_x and l_y are equal to $1/\rho_2$ and $1/\rho_1$, respectively. Note that oblique coordinate formulation is useful and tractable for applying the periodic boundary conditions to the obliquely crossed problem.

The θ-ply crack propagation along the fiber direction in $[0/\theta_2/90]_s$ laminates in the presence of developed 90-ply cracks is considered. Transverse cracks in a single-ply block induce matrix cracks in the adjacent plies under static or fatigue loadings, and in some cases, these cracks barely propagate in the fiber direction.[4,5] Thus, the mechanisms of microcrack formation are investigated in conjunction with changes in angle θ. Transverse stress distribution in the intact ply, that is, 0 ply, is also analyzed in connection with further multiple-ply crack accumulation.

Eight-node isoparametric elements are used in this study. Double nodes are arranged on the crack surfaces, and the θ-ply crack length is controlled by fixing the corresponding double nodes. The ply thickness is set to be 0.14 mm, and the material properties used here (IM600/133) are summarized in Table 1 referred to those of Aoki et al.[3] Note that temperature dependence is included using linear interpolation between the given temperatures, and stress-free and setting temperatures are assumed to be 100 and 20°C, respectively, unless otherwise noted. Energy release rates associated with θ-ply crack growth are calculated using the crack closure method. Crack densities that are defined in Fig. 5a are set as $\rho_1 = 5$ cm^{-1} and $\rho_2 = 2$ cm^{-1}.

As discussed in recent research,[16] delaminations between the cracked plies have significant effects on the propellant leakage. Although delaminations may be induced at the vicinity of obliquely crossed cracks, they are assumed to evolve beyond the θ-ply crack propagation. Therefore, the effect of delaminations on θ-ply crack propagation is neglected in this study, although this topic can be investigated if crack-tip delaminations are introduced in the present model.

Numerical Results

Induced Crack Growth in θ-Degree Ply

Calculated energy release rates are plotted as a function of normalized projected crack length (projected length a divided by θ-ply thickness) in Fig. 6 for the cases of $\theta = 30$ and 60 deg. The applied strains are determined under the conditions of uniaxial tension loadings in the 0-deg direction corresponding to 10,000 μ of undamaged laminates in the orthogonal coordinates. For comparison, the values associated with θ-ply crack growth without 90-ply cracks are also shown by solid (mode 1) and dashed (mode 2) lines. Note that the mode 3 components are negligible. In this paper, crack formation is assumed to be mainly attributed to mode 1 components because mode 2 fracture toughness is much higher than mode 1 toughness in the case of common polymer-based composites. Thus, mode 1 energy release rates are the focus of the following discussions. It can

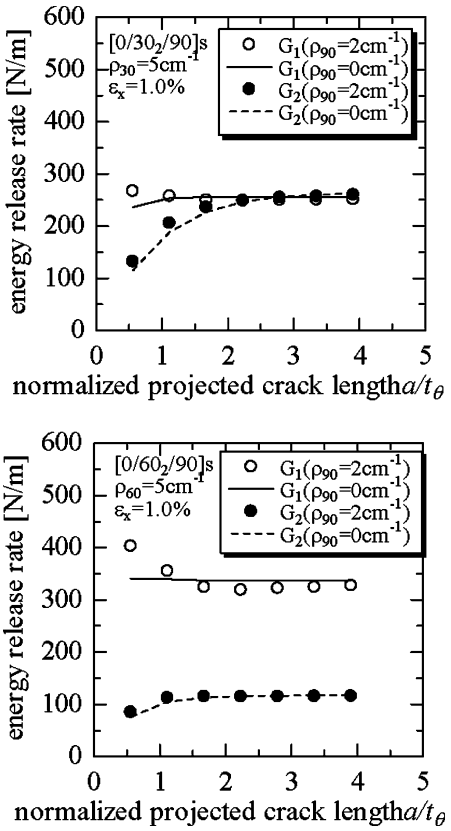

Fig. 6 Energy release rates associated with θ-ply crack propagation in $[0/\theta_2/90]_s$ laminates with $\theta = 30$ and 60; normalized projected crack length a/t_θ.

be seen that mode 1 energy release rates increase at the vicinity of the 90-ply cracks. To clarify the energy release rates when a/t_θ approaches zero, numerical results using fine meshes of $[0/60_2/90]_s$ laminates are shown in Fig. 7. Figure 7 indicates that mode 1 energy release rate decreases to zero when a/t_θ approaches zero and reveals the maximum value about at $a/t_\theta = 0.6$. When crack length increases, energy release rates reach steady state, which is common between the cases with and without 90-ply cracks as shown in Fig. 6. Additionally, the difference of mode 1 components between the maximum and saturated values becomes larger in conjunction with increase of angle θ. Because the maximum and saturated energy release rates calculated from the model with fine meshes show similar results as the model with course meshes, the energy release rates obtained from the course meshes are used in the following results.

To investigate the effect of angle θ on the difference of energy release rates, parametric analyses in the case of projected crack length $a/t_\theta = 0.6$ and $a/t_\theta = 3.3$ are performed, and the obtained mode 1 energy release rates as a function of angle θ are plotted in Fig. 8. The rise of the mode 1 component in the $a/t_\theta = 0.6$ case is recognized when angle θ becomes large. The large difference between the maximum and saturated energy release rates may cause the formation of microcracks or stitch cracks, whereas the small difference

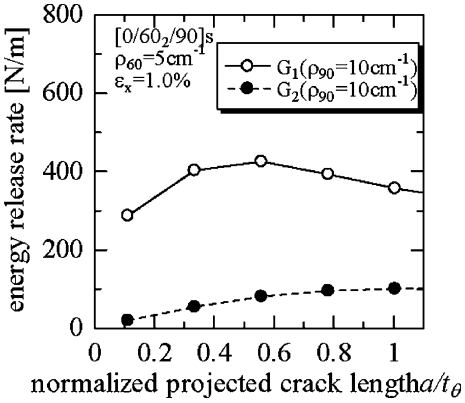

Fig. 7 Energy release rates associated with 60-ply crack propagation in $[0/60_2/90]_s$ laminates using fine meshes.

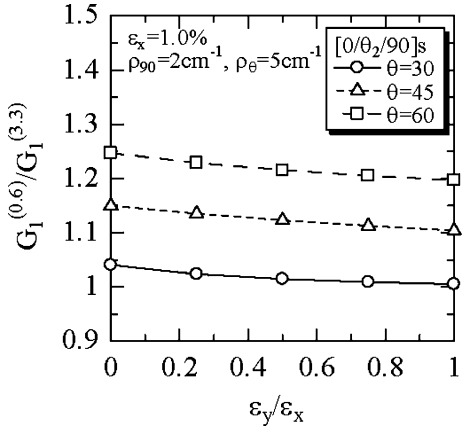

Fig. 10 Effect of strain level on energy release rate ratio.

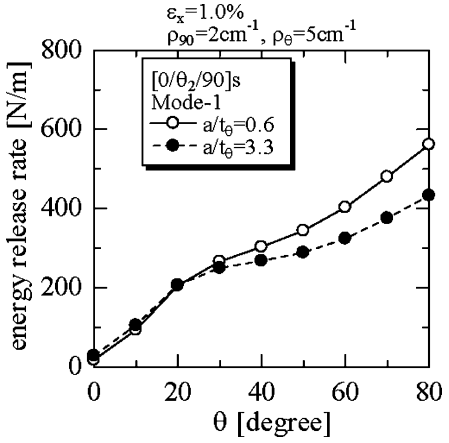

Fig. 8 Parametric analysis of energy release rates associated with θ-ply crack propagation in $[0/\theta_2/90]_s$ laminates when $a/t_\theta = 0.6$ and $a/t_\theta = 3.3$.

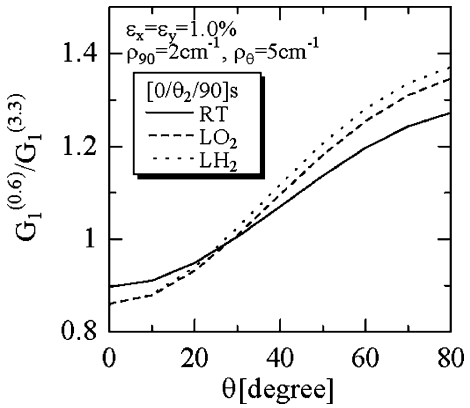

Fig. 11 Parametric analysis of energy release rates associated with θ-ply crack propagation: effect of cryogenic condition.

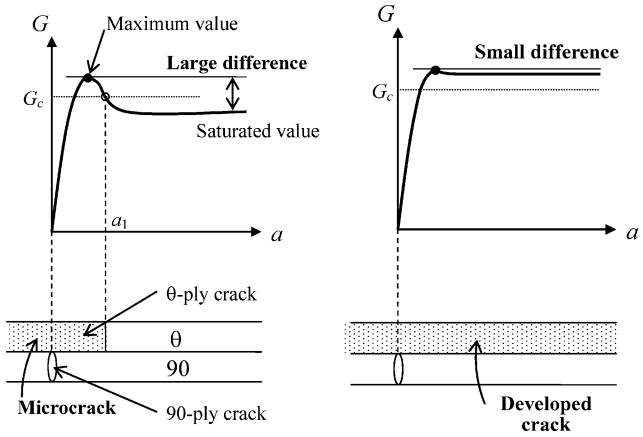

Fig. 9 Schematics of relationship between crack length and energy release rate rise.

results in formation of developed cracks because of unstable crack growth as shown in Fig. 9.

To investigate the applied strain levels on the difference of energy release rates, the energy release rate ratio (G_1 at $a/t_\theta = 0.6$ divided by G_1 at $a/t_\theta = 3.3$) is calculated when $\hat{\bar{\varepsilon}}_x = 10{,}000\ \mu$, $\hat{\bar{\varepsilon}}_y = R\bar{\varepsilon}_x$, and $\hat{\bar{\gamma}}_{xy} = 0$ (R varied) with some variety of angle θ as shown in Fig. 10. Although applied strains have some effects on the energy release rate difference, the trend of θ dependence is almost the same: Larger θ causes larger difference. Therefore, the susceptibility of stitch cracks (instead of propagation along the fiber direction) proves to depend mainly on the material and geometry, that is, elastic constants and angle θ, or the angle difference between the cracked and adjacent plies.

For cryogenic propellant tank application, the described parametric analysis at liquid oxygen (LO_2) (-183°C) and liquid hydrogen (LH_2) (-253°C) temperatures is also carried out for the condition $\hat{\bar{\varepsilon}}_x = 10{,}000\ \mu$, $\hat{\bar{\varepsilon}}_y = 10{,}000\ \mu$, and $\hat{\bar{\gamma}}_{xy} = 0$. The mode 1 energy release rates at $a/t_\theta = 0.6$ and $a/t_\theta = 3.3$ are calculated, and the energy release rate ratio (G_1 at $a/t_\theta = 0.6$ divided by G_1 at $a/t_\theta = 3.3$) as a function of angle θ is plotted in Fig. 11. It can be concluded that, although the energy release rate ratio is different among the three temperatures, the θ dependence shows a similar trend to that at room temperature even under cryogenic conditions. Thus, geometrical layups may primarily control adjacent-ply cracking modes, that is, stitch or developed cracks.

Transverse Stress in 0-Degree Ply

The 0-ply normal stress transverse to the fiber direction of $[0/\theta_2/90]_s$ laminates in the presence of 90- and θ-ply cracks is investigated. The analytical conditions are identical to those in the example shown in Fig. 6, and the θ-ply crack projected lengths are set as $a = 0.31$ mm and $a = 0.78$ mm. The 0-ply stress distribution (in-plane transverse to the 0-ply fiber direction) at $z = 0.455$ mm, where $z = 0$ corresponds to the middle surface of the laminate, in the case of $a = 0.31$ mm is shown in Fig. 12, which indicates that stress increases only at the vicinity of a θ-ply crack. Thus, comparison of cross-sectional stress distributions on $y = 0$ is shown in Fig. 13. It is concluded that the θ-ply crack length has little effect on the amount of 0-ply stress increase. This leads to the inference that a 0-ply crack may be induced irrespective of θ-ply cracking modes (stitch or developed cracks) once θ-ply cracks occur.

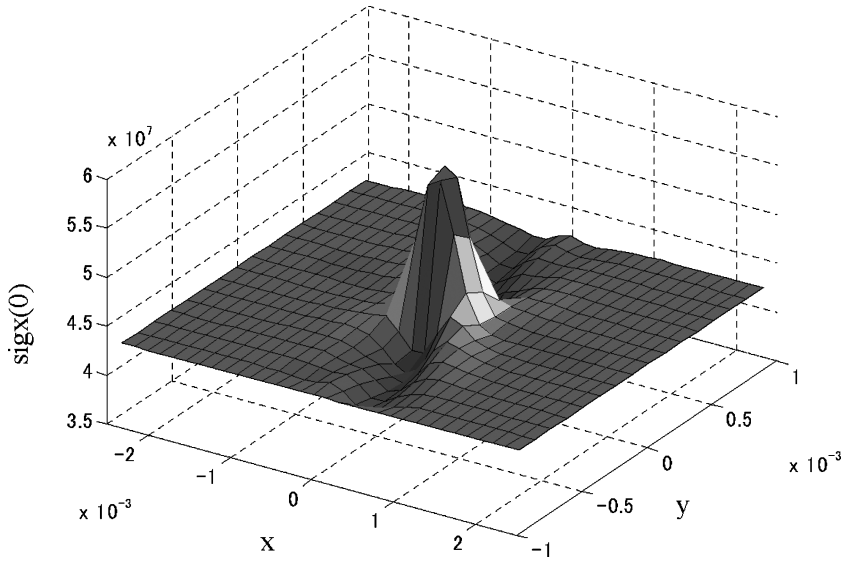

Fig. 12 Transverse stress distribution of 0 ply in $[0/\theta_2/90]_s$ laminate in the presence of obliquely crossed cracks: $a = 0.31$ mm.

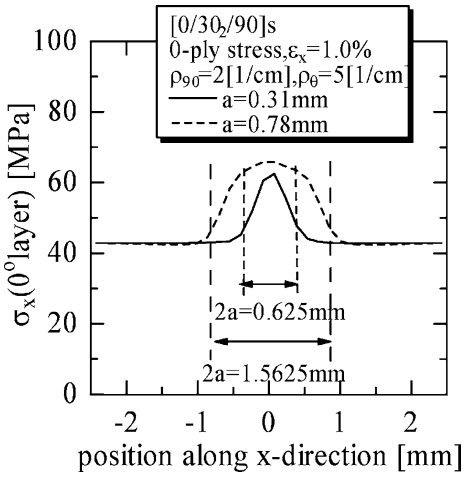

Fig. 13 Cross-sectional transverse stress distribution 0-ply in $[0/\theta_2/90]_s$ laminate in the presence of obliquely crossed cracks: $a = 0.31$ and 0.78 mm.

Note on Through-Thickness Connection of Matrix Cracks

Conventional two-dimensional analytical models can handle the developed cracks, but not the mentioned stitch cracks. The stitch cracks appear at lower strain levels than the fully developed cracks because of the increase in energy release rates at the vicinity of preexisting cracks, as indicated in the present study. Therefore, prediction of crack accumulation in multiple plies using analytical models may involve some risks for situations of microcracks or stitch cracks. However, the energy release ratio introduced in this study has potential for stitch cracking prediction because steady-state (or saturated) energy release rates can be evaluated using analytical models.

Through-thickness connection of matrix cracks, including both developed and stitch cracks, was experimentally observed and should be evaluated for propellant leakage problems. Composite laminates may be more susceptible to through-thickness connection of matrix cracks than one might imagine (or predict using conventional analytical models). However, because of the small damage size, the amount of leakage through stitch crack intersections is expected to be small compared to that in the case of developed cracks.

Conclusions

In this study, damage induction mechanisms of matrix cracks and through-thickness connection of matrix cracks were discussed based on both experimental and numerical studies, because related topics of composite propellant tank $[0/\theta_2/90]_s$ laminates suggested that layup angles have significant effects on the θ-ply crack induction mechanism. Microcracks or stitch cracks were observed in the case of small intersecting angles between θ- and 90-deg plies, whereas developed cracks were the main damage modes in the case of large intersecting angles. These phenomena could be explained by calculating energy release rates associated with θ-ply crack growth in the presence of matrix cracks in 90-deg plies. It was shown that an increase in energy release rates at the vicinity of 90-ply cracks causes microcrack formation instead of developed cracks and that the energy release rate ratios increase in conjunction with decrease of intersecting angle.

Further crack induction in the presence of matrix cracks in multiple plies was also investigated. It was concluded that, once cracks appear in a single-ply block, cracks may be induced in the adjacent plies irrespective to the length of the existing cracks. Composite laminates may be more susceptible to through-thickness connection of matrix cracks than one might imagine in the case of stitch crack accumulation. However, the energy release ratio introduced in this study, which can be regarded as a material/geometric parameter, has the potential for stitch cracking prediction because steady-state (or saturated) energy release rates can be evaluated using analytical models.

References

[1]Robinson, M. J., "Composite Cryogenic Propellant Tank Development," AIAA Paper 94-1375, April 1994.

[2]Robinson, M. J., Eichinger, J. D., and Johnson, S. E., "Hydrogen Permeability Requirements and Testing for Reusable Launch Vehicle Tanks," AIAA Paper 2002-1418, April 2002.

[3]Aoki, T., Ishikawa, T., Kumazawa, H., and Morino, Y., "Mechanical Performance of CF/Polymer Composite Laminates under Cryogenic Conditions," AIAA Paper 2000-1605, April 2000.

[4]Kumazawa, H., Aoki, T., and Susuki, I., "Analysis and Experiment of Gas Leakage Through Cross-Ply Laminates for Propellant Tanks," *AIAA Journal*, Vol. 41, No. 10, 2003, pp. 2037–2044.

[5]Gates, T. S., Grenoble, R., and Whitley, K. S., "Permeability and Lifetime Durability of Polymer Matrix Composites for Cryogenic Fuel Tanks," AIAA Paper 2004-1859, April 2004.

[6]Nairn, J. A., and Hu, S., "Micromechanics of Damage: A Case Study of Matrix Microcracking," *Damage Mechanics of Composite Materials*, edited by R. Talreja, Elsevier, Amsterdam, 1994, pp. 187–243.

[7]Nairn, J. A., "Matrix Microcracking in Composites," *Polymer Matrix Composites*, edited by R. Talreja and J. A. E. Manson, Elsevier, Amsterdam, 2000, pp. 403–432.

[8]Whitley, K. S., and Gates, T. S., "Thermal/Mechanical Response and Damage Growth in Polymeric Composites at Cryogenic Temperatures," AIAA Paper 2002-1416, April 2002.

[9]Bechel, V. T., Fredin, M. B., Donaldson, S. L., Kim, R. Y., and Camping, J. D., "Effect of Stacking Sequence on Micro-Cracking in a Cryogenically Cycled Carbon/Bismaleimide Composite," *Composites Part A*, Vol. 34, No. 7, 2003, pp. 663–672.

[10]Masters, J. E., and Reifsnider, K. L., "An Investigation of Cumulative Damage Development in Quasi-Isotropic Graphite/Epoxy Laminates," *Damage in Composite Materials*, ASTM STP, Vol. 775, American Society for Testing and Materials, 1982, pp. 40–61.

[11]Johnson, P., and Chang, F. K., "Characterization of Matrix Crack-Induced Laminate Failure—Part I: Experiments," *Journal of Composite Materials*, Vol. 35, No. 22, 2001, pp. 2009–2035.

[12]Lavoie, J. A., and Adolfsson, E., "Stitch Cracks in Constraint Plies Adjacent to a Cracked Ply," *Journal of Composite Materials*, Vol. 35, No. 23, 2001, pp. 2077–2097.

[13]Pagano, N. J., and Schoeppner, G. A., "Delaminations of Polymer Matrix Composites: Problems and Assessment," *Polymer Matrix Composites*, edited by R. Talreja and J. A. E. Manson, Elsevier, Amsterdam, 2000, pp. 433–528.

[14]Sun, C. T., and Chung, I., "An Oblique End-Tab Design for Testing Off-axis Composite Specimens" *Composites*, Vol. 24, No. 8, 1993, pp. 619–623.

[15]Yokozeki, T., Aoki, T., and Ishikawa, T., "Parametric Analysis on the Adjacent Ply Crack Formation in Laminated Structures for Cryogenic Propellant Tank Application," AIAA Paper 2004-1772, April 2004.

[16]Noh, J., Whitcomb, J., Peddiraju, P., and Lagoudas, D., "Prediction of Leakage Rate Through Damage Network in Cryogenic Composite Laminates," AIAA Paper 2004-1861, April 2004.

L. Peterson
Associate Editor